Joint Estimation of Timing and Carrier Phase Offsets for MSK Signals in Alpha-Stable Noise

Guosheng Yang, Jun Wang, *Member, IEEE*, Guoyong Zhang, Qijia Shao, and Shaoqian Li, *Fellow, IEEE*

***Abstract*— Impulsive noise modeled as symmetric α-stable (SαS) distribution is commonly seen in many practical communication scenarios. In this letter, we focus on the joint timing and carrier phase synchronization of minimum shift keying signals in SαS noise. We first derive the Cramér–Rao lower bound (CRLB) of joint timing and carrier phase offsets estimation. Then, an optimal synchronization training sequence is designed to minimize the CRLB. As the corresponding maximum likelihood estimator is hard to implement in SαS noise, we further propose a pragmatic synchronization parameters estimation algorithm based on explicit myriad cost function and a global optimization method. Extensive simulation results show that our proposed algorithm works well and is robust to the estimation errors of received signal-to-noise ratio and SαS noise parameter.**

***Index Terms*— Alpha-stable noise, synchronization, global optimization.**

I. Introduction

CLASSICAL communication techniques are mostly derived and designed under the assumption that noise follows Gaussian distribution. Nevertheless, in many scenarios, noises are commonly non-Gaussian and have distinct impulsive characteristic. For example, in very low frequency and low frequency (VLF/LF) communications and shallow underwater communications, impulsive noise is widely observed, meaning that some samples are much more severely corrupted than others [1]–[3]. Under such cases, applying Gaussian noise-based approaches often output poor results for signal processing tasks. As studied in [1]–[3], instead of using Gaussian model, using symmetric α-stable (SαS) distribution to model such impulsive noise is more appealing, since SαS distribution has a 'heavy tail' probability density function (PDF) which can better describe the pulses in impulsive noise.

Communication and signal processing techniques in SαS impulsive noise have garnered attention from the research community [2]–[6]. In this letter, we focus on the joint timing and carrier phase synchronization for minimum shift keying (MSK), since this modulation has been widely used in VLF/LF communications where SαS noise exists [1], [7]. Obviously, it is necessary to provide the synchronization performance bound in impulsive noise, based on which synchronization algorithms can be evaluated. Unfortunately, such performance bound analysis has not been addressed to the best of our knowledge. Note that MSK synchronization has been investigated in Gaussian noise [8]. In SαS noise, the basic principle of existing synchronization method is as follows: the received signal is first fed to a nonlinear pre-processing to suppress impulsive noise, then a synchronization method for Gaussian noise is performed [2], [9].

In this letter, we first derive the Cramér-Rao lower bound (CRLB) of joint estimation of timing and carrier phase offsets of MSK signals. Our derivation shows that the resulting CRLB is a function of the adopted synchronization training sequence (TS). Then, an optimal TS is further proposed to minimize the CRLB. To the best of our knowledge, the CRLB analysis and the design of optimal TS minimizing the CRLB have not been considered in impulsive noise. Next, we propose a pragmatic algorithm to estimate these two synchronization parameters. As its closed form can not be obtained, the maximum likelihood estimator (MLE) of the desired parameters is hard to implement. Then, we adopt an explicit myriad cost function for this estimation problem, and apply a global optimization method to solve it. It is worth noting that when the carrier frequency offset is considered, the proposed estimation algorithm can still work by a simple extension. The simulation results show that the performance gap between our proposed algorithm and the CRLB is negligible. We also investigate the sensitivity of the proposed algorithm to the estimation errors of the received signal-to-noise ratio (SNR) and SαS noise parameter α by extensive simulations. The results show that our proposed algorithm is robust under practical estimation errors of SNR and α.

II. Signal Model

In VLF/LF communications, MSK signals have been widely adopted, and the dominant atmospheric noise can be modeled by SαS distribution [1], [7]. Meanwhile, the propagation channel of VLF/LF communications can be considered to be frequency-flat [10]. We choose the Data-Aided (DA) synchronization, for which desired parameters are usually estimated based on the transmitted known TS [8]. Let $\{d_l\}$, $l = 0, \cdots, L-1$, T and T_s be the TS, the sampling interval and the symbol period of transmitted MSK signals, respectively. The received signal's complex baseband sample corresponding to the TS can be given by [8]

$$r_0(n) = \rho_{ch}\sqrt{P_s}e^{j\theta}e^{j\pi\sum_{l=0}^{L-1} d_l q(nT - lT_s - \tau T_s)} + v_0(n),$$

where $q(nT)$ is the phase response of MSK signals, which satisfies $q(nT) = nT/(2T_s)$ for $0 \le nT < T_s$ and $q(nT) = 1/2$ for $nT \ge T_s$. Moreover, P_s is the average power of transmitted

Manuscript received September 20, 2017; revised October 23, 2017; accepted October 23, 2017. Date of publication October 27, 2017; date of current version January 8, 2018. This work is supported in part by the National Natural Science Foundation of China (NSFC) under grant 61471099, the Application Fundamental Research Program of Sichuan Province under grant 2016JY0104, the Foundation of the National Key Laboratory of Science and Technology on Communications, National Defense Pre-Research Foundation of China. The associate editor coordinating the review of this paper and approving it for publication was L. Lampe. *(Corresponding author: Jun Wang.)*

The authors are with the National Key Laboratory of Science and Technology on Communications, University of Electronic Science and Technology of China, Chengdu 611731, China (e-mail: ygshmunity@163.com; junwang@uestc.edu.cn; 15882214708@163.com; qijiashao@gmail.com; lsq@uestc.edu.cn).

Digital Object Identifier 10.1109/LCOMM.2017.2767031

signals; ρ_{ch} represents the amplitude of channel fading, which remains constant during synchronization under the assumption of flat and slowly varying fading environments. The notations $\tau T_s \in [0, T_s)$ and $\theta \in [0, 2\pi)$ represent the unknown timing and carrier phase offsets, respectively. Additionally, $v_0(n)$ is the complex baseband sample of SαS noise. Let the subscript 'R' and 'I' denote the real and imaginary components of one variable, respectively. According to the baseband conversion scheme presented in [3], it can be assumed that $v_{0,R}(n)$ and $v_{0,I}(n)$ are independently and identically distributed (i.i.d.) mutually, and both of them follow i.i.d. SαS distribution. Here, the Gaussian noise, which usually models the background noise in communications, is not contained in noise model.

A SαS distribution has two parameters, i.e., the characteristic exponent $0 < \alpha \leq 2$ and the scale parameter $\gamma > 0$ [2]. A smaller α indicates that more distinguishable pulses exist. Except some special cases, the whole family of SαS distributions has no explicit PDF. But it has an explicit characteristic function (CF), which can be given by $\phi(w) = e^{-\gamma^{\alpha}|w|^{\alpha}}$ [2]. Let the characteristic exponent and scale parameter of $v_{0,R}(n)$ and $v_{0,I}(n)$ be α and γ, respectively. The SNR of received signals can be defined as

$$\eta = \rho_{ch}^2 P_s / \gamma^2.$$

Then, we can adopt the following power-normalized equivalent receiver model for convenience,

$$r(n) = \underbrace{\sqrt{\eta} e^{j\theta} e^{j\pi \sum_{l=0}^{L-1} d_l q(nT - lT_s - \tau T_s)}}_{s(n,\mathbf{p})} + v(n), \tag{1}$$

where $\mathbf{p} = [p_1, p_2]^T = [\tau, \theta]^T$ is the desired parameter vector for synchronization, and $v(n) = v_0(n)/\gamma$ is the equivalent complex baseband SαS noise, whose real and imaginary components have normalized scale parameters.

III. Cramér-Rao Lower Bound Analysis

In this section, we analyze the CRLB of estimating $\mathbf{p}$. Denote the vectors $\mathbf{r} = [r_n]^T = [r(n)]^T$, $\mathbf{s} = [s_n]^T = [s(n, \mathbf{p})]^T$, $\mathbf{e} = \mathbf{r} - \mathbf{s} = [e_n]^T$, where $n = 0, \cdots, N-1$, and N is the number of samples of received signals during synchronization. Then, the logarithmic likelihood function (LLF) used to estimate $\mathbf{p}$ can be given by

$$\Lambda(\mathbf{r}, \mathbf{p}) = \sum_{n=0}^{N-1} \left[\ln f\left(e_{n,R}\right) + \ln f\left(e_{n,I}\right) \right].$$

Based on our defined noise model, $e_{n,R}$ and $e_{n,I}$ follow i.i.d. SαS distribution with character exponent α and scale parameter 1; $f(\cdot)$ denotes the same PDF of $e_{n,R}$ and $e_{n,I}$.

The Fisher Information Matrix (FIM) $\mathbf{I}(\mathbf{p}) \in \mathbb{R}^{\mathbf{2\times 2}}$ of estimating $\mathbf{p}$ can be derived by [11]

$$\begin{aligned}
&\left[\mathbf{I}(\mathbf{p})\right]_{i,j} \\
&= -\mathrm{E}\left\{ \left[\frac{\partial \Lambda(\mathbf{r}, \mathbf{p})}{\partial p_i} \right] \left[\frac{\partial \Lambda(\mathbf{r}, \mathbf{p})}{\partial p_j} \right]^T \right\} \\
&= \sum_{n=0}^{N-1} \left\{ \frac{\partial s_{n,R}}{\partial p_i} \frac{\partial s_{n,R}}{\partial p_j} \mathrm{E}\left[g'(e_{n,R}) \right] + \frac{\partial s_{n,I}}{\partial p_i} \frac{\partial s_{n,I}}{\partial p_j} \mathrm{E}\left[g'(e_{n,I}) \right] \right\} \\
&\quad - \sum_{n=0}^{N-1} \left\{ \frac{\partial^2 s_{n,R}}{\partial p_i \partial p_j} \mathrm{E}\left[g\left(e_{n,R}\right) \right] + \frac{\partial^2 s_{n,I}}{\partial p_i \partial p_j} \mathrm{E}\left[g\left(e_{n,I}\right) \right] \right\},
\end{aligned} \tag{2}$$

where $i, j = 1, 2$, and $g(x)$ is the score function of SαS distribution with the following form [2],

$$g(x) = -f'(x)/f(x).$$

It has been known that when x approaches infinity, the PDF $f(x)$ satisfies $f(x) \sim (\alpha C_\alpha / 2) x^{-\alpha-1}$, where C_α is a constant determined by α, and the notation '$\sim$' stands for the asymptotic equivalence relation [2]. Then, the expectation presented in Eq. (2) can be obtained as follows,

$$\begin{aligned}
\mathrm{E}\left[g\left(e_{n,R}\right) \right] &= \int_{-\infty}^{\infty} g\left(e_{n,R}\right) f\left(e_{n,R}\right) de_{n,R} \\
&= -\left[f\left(e_{n,R}\right) \right]_{-\infty}^{\infty} = 0.
\end{aligned}$$

Meanwhile, $\mathrm{E}[g'(e_{n,R})]$ can also be given as

$$\begin{aligned}
\mathrm{E}\left[g'\left(e_{n,R}\right) \right] &= \int_{-\infty}^{\infty} g'\left(e_{n,R}\right) f\left(e_{n,R}\right) de_{n,R} \\
&= \underbrace{\int_{-\infty}^{\infty} \left[f'\left(e_{n,R}\right) \right]^2 / f\left(e_{n,R}\right) de_{n,R}}_{\kappa(\alpha)}.
\end{aligned}$$

Similarly, we have $\mathrm{E}\left[g\left(e_{n,I}\right) \right] = 0, \mathrm{E}\left[g'\left(e_{n,I}\right) \right] = \int_{-\infty}^{\infty} \left[f'\left(e_{n,I}\right) \right]^2 / f\left(e_{n,I}\right) de_{n,I} = \kappa(\alpha)$. Then, we can have

$$\left[\mathbf{I}(\mathbf{p})\right]_{i,j} = \kappa(\alpha) \sum_{n=0}^{N-1} \left[\frac{\partial s_{n,R}}{\partial p_i} \frac{\partial s_{n,R}}{\partial p_j} + \frac{\partial s_{n,I}}{\partial p_i} \frac{\partial s_{n,I}}{\partial p_j} \right]. \tag{3}$$

By substituting the expressions of MSK signals presented in Eq. (1) into Eq. (3), the CRLB of estimating $[\tau, \theta]^T$ can be given by

$$\begin{aligned}
\mathrm{CRLB}\{\tau\} &= \left[\mathbf{I}^{-1}(\mathbf{p}) \right]_{1,1} \\
&= \frac{4}{\pi^2} \cdot \frac{1}{\eta \kappa(\alpha) N} \cdot \frac{1}{1 - \left(\sum_{l=0}^{L-1} d_l / L \right)^2}, \\
\mathrm{CRLB}\{\theta\} &= \left[\mathbf{I}^{-1}(\mathbf{p}) \right]_{2,2} = \frac{1}{\eta \kappa(\alpha) N} \cdot \frac{1}{1 - \left(\sum_{l=0}^{L-1} d_l / L \right)^2}.
\end{aligned}$$

Note that $\kappa(\alpha)$ reveals the effect of parameter α on the CRLB. Based on the characteristic of $\kappa(\alpha)$, with the decrease of α, the CRLB changes little when $\alpha \geq 1$, but falls rapidly when $\alpha < 1$. Meanwhile, larger sample number N, e.g., larger oversampling rate, can lead to smaller CRLB. Furthermore, as the CRLB is a function of TS $\{d_l\}$, we can give an optimal TS to minimize the CRLB. Obviously, the optimal TS should satisfy

$$\sum_{l=0}^{L-1} d_l = 0. \tag{4}$$

IV. Synchronization Algorithm Design

In this section, an estimation algorithm of the synchronization parameter vector $\mathbf{p} = [\tau, \theta]^T$ is proposed. The estimation of $\mathbf{p}$ is the solution of the following optimization problem,

$$\begin{aligned}
\hat{\mathbf{p}} = \ & \arg\min_{\{\mathbf{p}\}} J(\mathbf{r}, \mathbf{p}) \\
& \text{s.t.} \quad 0 \leq \tau < 1, 0 \leq \theta < 2\pi,
\end{aligned} \tag{5}$$

where $J(\mathbf{r}, \mathbf{p})$ is the adopted cost function. The optimal cost function can be designed based on the LLF, then the MLE

is obtained. Unfortunately, the LLF has no closed form and thus the MLE is hard to implement in SαS noise. To design an easily implementable algorithm, we propose to employ the myriad cost function, which has a closed form. Comparing with the optimal LLF based cost function, the myriad cost function has near-optimal performance and has been used for the adaptive filter and signal detection in SαS noise [4], [5]. The myriad cost function can be formulated as follows,

$$J(\mathbf{r},\mathbf{p}) = \sum_{n=0}^{N-1} \ln\left[K^2 + (r_R(n) - s_R(n,\mathbf{p}))^2\right] + \sum_{n=0}^{N-1} \ln\left[K^2 + (r_I(n) - s_I(n,\mathbf{p}))^2\right], \quad (6)$$

where the tunable parameter K can make the cost function adapt different cases of SαS distribution, and can be calculated empirically via $K = \sqrt{\alpha/(2-\alpha)}$ [4], [5].

On the basis of [5], the myriad cost function may be non-convex, implying that the global search method is recommended to handle the optimization problem Eq. (5). Here we adopt a typical global search method, i.e., the Branch-and-Bound algorithm [12]. In Branch-and-Bound algorithm, the search space of $\mathbf{p}$ is first split into multiple sub-regions. For a sub-region, if it potentially contains the globally optimal solution, it will continue to be split, or else, it will be deleted. The key of the Branch-and-Bound algorithm is to give a bound function of $J(\mathbf{r},\mathbf{p})$ in a sub-region. In what follows, the Lipschitz constant based lower bound will be derived.

It has been known that the search space of $\mathbf{p}$ is a rectangle region, thus we can split the search space into some small sub-rectangle regions, and each of vertices of the sub-rectangle corresponds to a vector $\mathbf{p}$. The following proposition gives a Lipschitz constant based lower bound of $J(\mathbf{r},\mathbf{p})$ in a sub-rectangle region.

Proposition 1: Let $\mathbf{p_1}$ and $\mathbf{p_2}$ represent a pair of diagonal vertices of a sub-rectangle region, then the Lipschitz constant based lower bound of $J(\mathbf{r},\mathbf{p})$ in this region can be given by

$$J(\mathbf{r},\mathbf{p}) \geq \frac{J(\mathbf{r},\mathbf{p}_2) + J(\mathbf{r},\mathbf{p}_1)}{2} - C\frac{\|\mathbf{p}_2 - \mathbf{p}_1\|}{2}, \quad (7)$$

where the Lipschitz constant C is

$$C = \sqrt{\eta\left(\pi^2/4+1\right)}\sum_{n=0}^{N-1}\left(\frac{2|r_R(n)|}{K^2 + r_R^2(n)} + \frac{2|r_I(n)|}{K^2 + r_I^2(n)}\right).$$

Proof: Let us denote

$$J_{n,R}(\mathbf{r},\mathbf{p}) = \ln\left[K^2 + (r_R(n) - s_R(n,\mathbf{p}))^2\right].$$

In the sub-rectangle region with a pair of diagonal vertices $\mathbf{p_1}$ and $\mathbf{p_2}$, the Lipschitz constant based lower bound of $J_{n,R}(\mathbf{r},\mathbf{p})$ can be given as [12]

$$J_{n,R}(\mathbf{r},\mathbf{p}) \geq \frac{J_{n,R}(\mathbf{r},\mathbf{p}_2) + J_{n,R}(\mathbf{r},\mathbf{p}_1)}{2} - C_{n,R}\frac{\|\mathbf{p}_2 - \mathbf{p}_1\|}{2}. \quad (8)$$

Here $C_{n,R}$ is the corresponding Lipschitz constant, which can be calculated as the supremum of $\|\partial J_{n,R}(\mathbf{r},\mathbf{p})/\partial\mathbf{p}\|$ [12]. Meanwhile, we have

$$\|\partial J_{n,R}(\mathbf{r},\mathbf{p})/\partial\mathbf{p}\| = \left|\partial J_{n,R}(\mathbf{r},\mathbf{p})/\partial s_R(n,\mathbf{p})\right| \cdot |s_I(n,\mathbf{p})| \cdot \sqrt{\pi^2/4+1},$$

where

$$\left|\partial J_{n,R}(\mathbf{r},\mathbf{p})/\partial s_R(n,\mathbf{p})\right| = \frac{2|r_R(n) - s_R(n,\mathbf{p})|}{K^2 + (r_R(n) - s_R(n,\mathbf{p}))^2}.$$

In VLF/LF communication scenarios, the amplitude of the impulsive noise is commonly much larger than that of the transmitted signal [9], [10]. In this case, we have the following result,

$$\|\partial J_{n,R}(\mathbf{r},\mathbf{p})/\partial\mathbf{p}\| \approx \frac{2|r_R(n)|\sqrt{\eta - s_R^2(n,\mathbf{p})}}{K^2 + r_R^2(n)} \cdot \sqrt{\pi^2/4+1}.$$

Finally, $C_{n,R}$ can be derived as

$$C_{n,R} = \frac{2|r_R(n)|}{K^2 + r_R^2(n)} \cdot \sqrt{\eta\left(\pi^2/4+1\right)}.$$

Similarly, the Lipschitz constant based lower bound of $J_{n,I}(\mathbf{r},\mathbf{p}) = \ln\left[K^2 + (r_I(n) - s_I(n,\mathbf{p}))^2\right]$ can also be given. Finally, the Lipschitz constant based lower bound of $J(\mathbf{r},\mathbf{p})$ can be obtained as Eq. (7). ■

By employing the above mentioned Branch-and-Bound algorithm, a synchronization algorithm is proposed in the following Algorithm 1.

Algorithm 1 Synchronization Algorithm

Input: R: the search space; ε: the stop criterion.
Output: $\hat{\mathbf{p}}$: the solution of the problem in Eq. (5).

1: Split R into four equal-area sub-rectangle regions, which are $\bar{R}_1, \bar{R}_2, \bar{R}_3, \bar{R}_4$; initialize $Q = \{\bar{R}_1, \bar{R}_2, \bar{R}_3, \bar{R}_4\}$, $J_m = \infty$, $\hat{\mathbf{p}} = [0,0]^T$;
2: **while** Q is not empty, **do**
3: choose a sub-rectangle region $\bar{R}_i$ from Q arbitrarily;
4: **if** both the length and width of $\bar{R}_i$ are less than ε, **then**
5: let $\hat{\mathbf{p}}_0$ be one of $\bar{R}_i$'s vertices;
6: **if** $J(\mathbf{r},\hat{\mathbf{p}}_0) < J_m$, **then**
7: $J_m = J(\mathbf{r},\hat{\mathbf{p}}_0)$, $\hat{\mathbf{p}} = \hat{\mathbf{p}}_0$;
8: **end if**
9: **else**
10: estimate $J(\mathbf{r},\mathbf{p})$'s lower bound J_{LB} using (7);
11: **if** $J_{LB} < J_m$, **then**
12: let Ω be the set of $\bar{R}_i$'s vertices;
13: $\hat{\mathbf{p}}_0 = \arg\min_{\mathbf{p}\in\Omega} J(\mathbf{r},\mathbf{p})$;
14: **if** $J(\mathbf{r},\hat{\mathbf{p}}_0) < J_m$, **then**
15: $J_m = J(\mathbf{r},\hat{\mathbf{p}}_0)$, $\hat{\mathbf{p}} = \hat{\mathbf{p}}_0$;
16: **end if**
17: split $\bar{R}_i$ into four equal-area sub-rectangles;
18: insert this four sub-rectangle regions into Q;
19: **end if**
20: **end if**
21: delete $\bar{R}_i$ from Q.
22: **end while**

1) Complexity: For the proposed algorithm, the computation complexity is determined by Step 3-21 and the number of iterations. In Step 3-21, the main computational burden is introduced by the calculation of myriad cost function $J(\mathbf{r},\mathbf{p})$. $J(\mathbf{r},\mathbf{p})$ needs to be calculated 8 times in Step 3-21. Based on Eq. (6), computing $J(\mathbf{r},\mathbf{p})$ requires $4N$ additions, $2N$ multiplications and $2N$ logarithmic operations. Meanwhile, extensive simulations show that dozens of iterations of Step 3-21 can guarantee the proposed algorithm to converge.

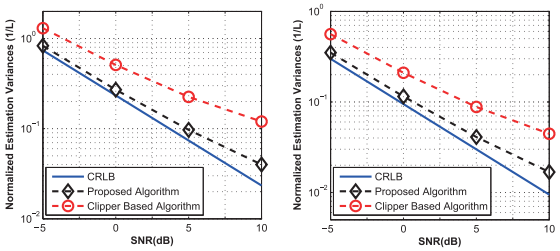

Fig. 1. The comparison between the CRLB and estimation variances of the proposed and the Clipper based algorithms for θ (left) and τ (right).

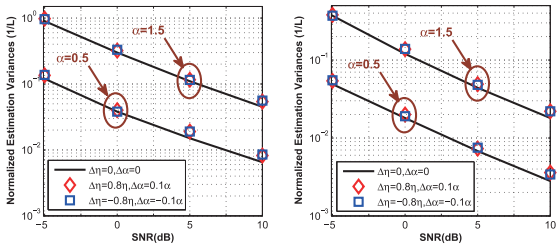

Fig. 2. The comparison between the estimation variances of θ (left) and τ (right) under different $\Delta\eta$ and $\Delta\alpha$.

2) Robustness: To perform the proposed synchronization algorithm, it is necessary to estimate received SNR η and parameter α of SαS noise. In practice, parameters η and α can be estimated by some synchronization-independent methods, e.g., the empirical characteristic function (ECF) based method [6]. We denote their estimations as $\hat{\eta} = \eta + \Delta\eta$ and $\hat{\alpha} = \alpha + \Delta\alpha$, respectively. By using the ECF based method, our simulations show that practical estimation errors can satisfy $|\Delta\eta| < 0.8\eta$ and $|\Delta\alpha| < 0.1\alpha$ by employing 2000 received symbols. The effects of $\Delta\eta$ and $\Delta\alpha$ on the proposed algorithm will be investigated by simulations in Section V.

V. Simulation Results

A point-to-point VLF/LF communication system is considered in our simulation, where MSK signals and SαS noise are adopted. The number of symbols in a TS is set to be $L = 20$. The timing offset τT_s and carrier phase offset θ are set to cover the intervals $[0, T_s)$ and $[0, 2\pi)$ uniformly, respectively. We present the synchronization performance in terms of the above defined SNR η. Besides, we choose the designed optimal TS based on Eq. (4) to make the CRLB reach the minimum. The stopping criterion in Algorithm 1 is set to be $\varepsilon = 0.001$.

In SαS noise, the existing synchronization algorithm includes a nonlinear pre-processing followed by a Gaussian based synchronization [2], [9]. Due to the extensive usage of the Clipper, it is chosen as the nonlinear pre-processing [2], [9]. The existing synchronization is called as Clipper based algorithm here. Based on [8], in Gaussian noise, Gaussian based synchronization can be given as $\hat{\mathbf{p}} = \arg\max_{\{\mathbf{p}\}} \mathrm{Re}\left[\sum_{n=0}^{N-1} r(n)\, s^*(n, \mathbf{p})\right]$.

The CRLB and estimation variances of the proposed and the existing Clipper based algorithms are compared in Fig. 1. The parameter α and the oversampling rate T_s/T are set to be 1.5 and 10, respectively. We can see that the proposed algorithm has significant performance gain than the Clipper based algorithm, and the former has negligible performance gap with the CRLB. The reason is that the used myriad cost function has near-optimal performance in SαS noise.

The estimation variances of the proposed and the Clipper based algorithms are also evaluated under different oversampling rates. Due to the page space constraint, corresponding simulation results are not illustrated in this letter. The results show that lower oversampling rate will lead to performance degradation for both our proposed and the Clipper based algorithms. This result is consistent with our CRLB analysis. Moreover, our proposed algorithm significantly outperforms the Clipper based algorithm under different oversampling rates. As lower oversampling rate means lower implementation complexity, a tradeoff between these two factors can be considered in practice.

Fig. 2 presents the comparison between the estimation variances of θ and τ under different estimation errors $\Delta\eta$ and $\Delta\alpha$. It can be observed that the practical estimation errors $\Delta\eta$ and $\Delta\alpha$, which are set according to the practical estimation performances of η and α using the above mentioned ECF based method, have negligible influence on the proposed algorithm.

VI. Conclusion

In this letter, we considered the synchronization of MSK signals in impulsive noise, which is modeled as SαS distribution. We derived the CRLB of the joint estimation of two key parameters in the synchronization, namely, the timing and carrier phase offsets. An optimal TS was further designed to minimize the CRLB. We also proposed an easily implementable synchronization algorithm based on the myriad cost function and the Branch-and-Bound algorithm. Simulation results verified that the proposed algorithm can achieve near-optimal performance comparing with the CRLB. Simulation results also validated that the proposed algorithm is robust to the practical estimation errors of SNR and noise parameter.

References

[1] D. A. Chrissan and A. C. Fraser-Smith, "A comparison of low-frequency radio noise amplitude probability distribution models," *Radio Sci.*, vol. 35, no. 1, pp. 195–208, 2000.
[2] C. L. Nikias and M. Shao, *Signal Processing with Alpha-Stable Distributions and Applications*. New York, NY, USA: Wiley, 1995.
[3] A. Mahmood, M. Chitre, and M. A. Armand, "On single-carrier communication in additive white symmetric alpha-stable noise," *IEEE Trans. Commun.*, vol. 62, no. 10, pp. 3584–3599, Oct. 2014.
[4] T. S. Saleh, I. Marsland, and M. El-Tanany, "Suboptimal detectors for alpha-stable noise: Simplifying design and improving performance," *IEEE Trans. Commun.*, vol. 62, no. 10, pp. 2982–2989, Oct. 2012.
[5] S. Kalluri and G. R. Arce, "Robust frequency-selective filtering using weighted myriad filters admitting real-valued weights," *IEEE Trans. Signal Process.*, vol. 49, no. 11, pp. 2721–2733, Nov. 2001.
[6] V. G. Chavali and C. R. C. M. da Silva, "Detection of digital amplitude-phase modulated signals in symmetric alpha-stable noise," *IEEE Trans. Commun.*, vol. 60, no. 11, pp. 3365–3375, Nov. 2012.
[7] K. Wiklundh, K. Fors, and P. Holm, "A log-likelihood ratio for improved receiver performance for VLF/LF communication in atmospheric noise," in *Proc. IEEE MILCOM*, Tampa, FL, USA, Oct. 2015, pp. 1120–1125.
[8] U. Mengali and A. N. D'Andrea, *Synchronization Techniques for Digital Receivers*. New York, NY, USA: Springer, 1997.
[9] D. A. Chrissan, "Statistical analysis and modeling of low-frequency radio noise and improvement of low-frequency communications," Ph.D. dissertation, Dept. Elect. Eng., Univ. Stanford, Stanford, CA, USA, 1998.
[10] A. D. Watt, A. L. Cullen, V. A. Fock, and J. R. Wait, *VLF Radio Engineering*. New York, NY, USA: Pergamon, 1967.
[11] S. M. Kay, *Fundamentals of Statistical Signal Processing: Estimation*, vol. 1. Englewood Cliffs, NJ, USA: Prentice-Hall, 1993.
[12] J. D. Pintér, *Global Optimization in Action*. Norwell, MA, USA: Kluwer, 1996.